DESIGN OF PHOTON BEAMLINES AT THE EUROPEAN XFEL

Harald Sinn, Shafagh Dastjani-Farahani, Idoia Freijo-Martin, Germano Galasso, Jérôme Gaudin, Liubov Samoylova, Antje Trapp, Fan Yang

European XFEL, Albert-Einstein-Ring 19, 22765 Hamburg, Germany

Abstract

The European XFEL will provide up to 2700 X-ray pulses in trains of 600 microsecond duration at a repetition rate of 10 Hz. This leads to a short time heat load of more than 10 kW in a sub-mm spot on the optical elements averaged over a pulse train. In addition, the first optical elements are exposed to the less collimated high energy spontaneous radiation of similar magnitude. On the other hand, the conservation of coherence properties requires a stability of X-ray optics on the nanometer scale. The conceptual design of the two hard X-ray photon beamlines and the photon distribution scheme to different experimental stations is presented. Photon damage and heat load issues are discussed in the context of conceptual design aspects for mirrors and apertures.

INTRODUCTION

Starting operations in 2014, the European XFEL will add significant new capabilities to the field of X-ray lasers. Due to its superconducting accelerator technology, X-ray pulses can be produced in powerful bursts, where many thousand X-ray pulses of mJ-power and fs-durations can be produced in less than a millisecond. The average X-ray power during these bursts exceeds other X-ray lasers sources and storage ring facilities by many orders of magnitude and will enable new fields of research.

A particular challenge is the X-ray optics, which has to withstand these high power levels, but also conserve the coherence properties of the SASE beam. Also, the beamlines should be fairly flexible with respect to transmitted photon energies and power, since new emerging science applications might change the requirements to the X-ray optics in the course of the operation phase. In this report, current concepts of beam transport and beam distribution to several experimental stations are presented for the two hard X-ray beamlines SASE1 and SASE2 (see figure 1). The emphasis of the discussion is here on mirrors, which are the most essential and demanding optical elements of the photon beamlines. Their positions in the photon tunnels are mainly driven by the FEL beam divergences. Heat load and damage issues are further boundary conditions that have to be taken into account in the selection of mirror coatings and cooling concepts.

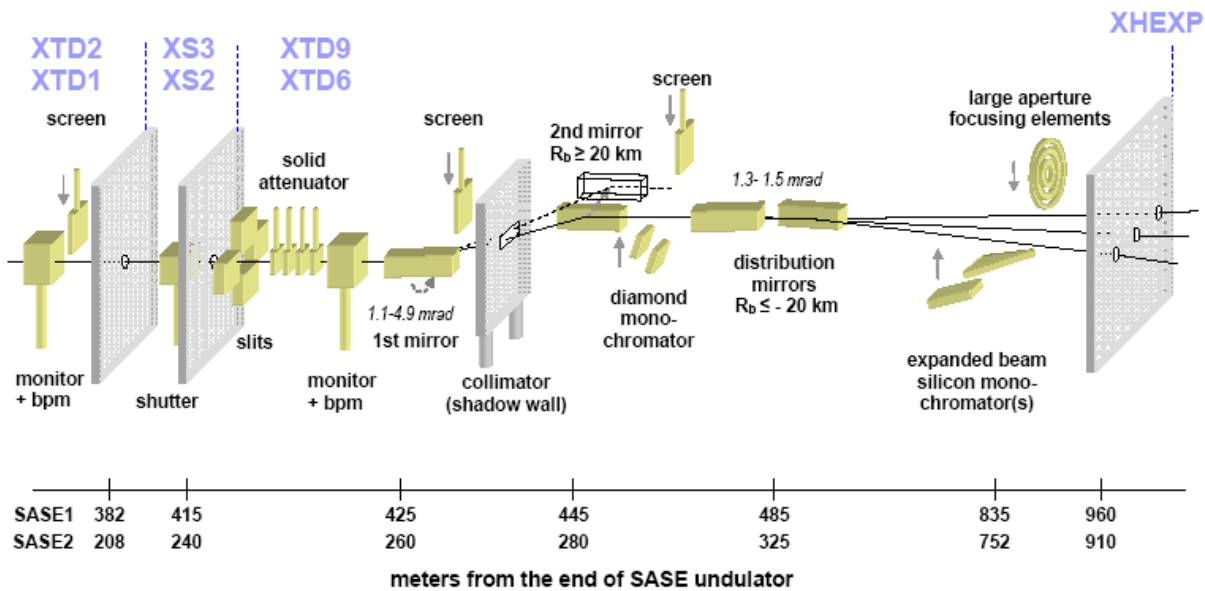

Figure 1: Layout of the SASE1&2 photon beamlines.

THE PHOTON DISTRIBUTION SYSTEM

In the XFEL technical design report from 2006 [1] the hard X-ray photon beamlines SASE1&2 have the task to transport FEL radiation from the undulators to the experimental hall ranging from 3 keV to 12 keV. However, since the undulators are gap-tunable, the upper limit of the FEL photon energy will depend among other parameters on the achievable slice emittance at the electron gun. Recent progress at LCLS [2] and DESY indicates that the FEL fundamental energies may reach 20 keV or higher. For the photon beamlines this means a large range of transmitted photon energies is required, while flux and coherence properties should be conserved as much as possible and damage to the optical elements is avoided.

Practical limitations are set by the length of available mirrors and possible locations of these mirrors in the photon tunnels. The wavefront of coherent SASE radiation is very sensitive to height errors on the mirror surface in the range of a few nanometers on all length scales [3, 4, and 5]. These stringent requirements can be fulfilled today only by few mirror manufacturers worldwide for mirror lengths below 500 mm by deterministic polishing techniques. Here, we assume in the conceptual design that the mirror polishing technology will evolve further over the next years, so that flat, deterministically polished mirrors with optical lengths up to 800 mm will be available for the photon distribution systems at the European XFEL.

The conceptual designs of the SASE1&2 photon beamlines are shown in figure 1. They differ only in the distances of optical elements from the end of the undulators. The upstream tunnels XTD2 and XTD1 and the shaft buildings XS3 and XS2 will also host undulators and electron beamlines. The available space for X-ray optics in these locations is limited and a relatively high radiation background will arise from the bending magnets in the shaft buildings. Therefore, only the minimum required diagnostics, passive apertures and shutters will be placed here. The tunnels containing the most and most sensitive of the photon beamline components are XTD9 for SASE1 and XTD6 for SASE2. After adjustable Bremsstrahlung apertures and solid attenuators a pair of horizontally deflecting mirrors will offset the FEL beam by 50 mm for radiation safety purposes. The beam will then either reach the middle beamline of the three possible beam locations in the experimental hall (building XHEXP) or will be deflected by another horizontally deflecting mirror to one of the branch stations, 1.45 m apart from the central beam position. A diamond monochromator is foreseen after the two offset mirrors, while silicon monochromators can be placed a few hundred meters downstream, where the heat load per area can be significantly reduced by beam expansion via bendable mirrors. Focusing optics will be placed 100 m or less in front of the experimental hall, or – for micron-sized or smaller foci – directly at the experiments.

Estimation of Mirror Lengths

Since the FEL beam from the undulators is almost diffraction limited and the source size depends only weakly on photon energy, the divergence of FEL radiation increases approximately linear with the photon wavelength in the hard X-ray regime. For optimization of beamline mirrors we approximate the energy dependence of the beam divergence of SASE1 and SASE2 from 3-20 keV by:

$$\delta\theta_{FWHM}[\mu\text{rad}] = \frac{25.5}{E[\text{keV}]} \qquad (1)$$

Equation (1) is adjusted to the typical divergences of about 3 µrad FWHM at 8.3 keV observed during the commissioning phase of the LCLS in 2009. It exceeds the calculated beam divergences for the European XFEL in [1] by about a factor of two and more recent estimates [6] for a reduced slice emittance and lower bunch charge by about 50%. However, further improvements of electron gun emittance and betatron oscillations in the undulator section could increase the actual X-ray beam divergence over calculated values. Therefore, a safety margin in the divergence, as provided by equation (1), is desirable for the determination of mirror lengths.

Another important parameter is the maximum incident angle against the mirror surface, at which desired photon energy can be deflected. This so-called critical angle of total reflection is in the considered photon energy range roughly proportional to the photon wavelength. In figure 2, the critical angle in dependence of photon energy is plotted for different considered coating materials. An incident angle α, at which all these materials would reflect, is given by the relation

$$\theta[\text{mrad}] = \frac{27.0}{E[\text{keV}]} \qquad (2)$$

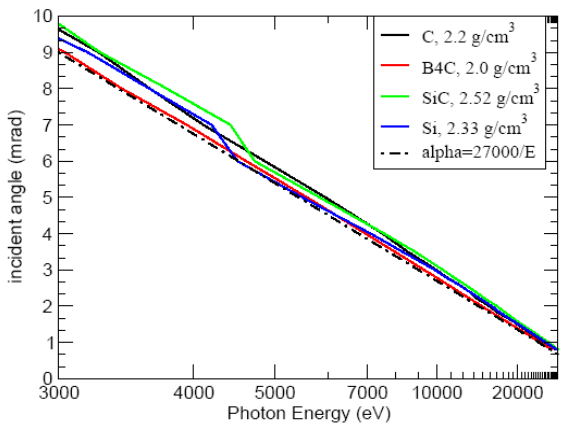

Figure 2: Critical angle for different coating materials plotted against the photon energy. The dashed-dotted curve represents the incident angles given by eq. (2).

Finally, the question arises, how much of the beam cross section should be reflected by the mirrors. A too short mirror will cut the number of transmitted photons and – due to the coherence of the FEL beam – will produce significant diffraction effects.

In figure 3, the latter effect is shown for the first offset mirror at SASE1 for 12.3 keV radiation: For projected mirror lengths of 6σ (d) and 5σ (c) of the FEL beam, distortions are very small and comparable to distortions from surface imperfections of deterministically polished mirrors [4]. A 4σ (b) projected mirror length will significantly distort the beam, but still produce a continuous beam spot, while reducing the length towards 2σ (a) will lead to breaking up of the beam profile and also significant loss of intensity.

As a design goal, we aim here for projected mirror lengths between 4σ and 6σ of the beam profile. If the mirror is set for one particular energy to the maximum possible incident angle according to eq. (2), the required mirror lengths be calculated as

$$l_{mirror} = \frac{s\ D_{source}\ \delta\theta_{FWHM}}{2\sqrt{2\ln 2}\sin\theta}$$

$$l_{mirror}[\mathrm{mm}] = 0.4\ s[\sigma]\ D_{source}[\mathrm{m}] \qquad (3)$$

with s = 4, 6 for a projected mirror length of 4σ or 6σ respectively. The minimum required lengths for the first offset mirrors for a single energy is are shown in table 1.

Table 1: Required minimum mirror lengths of the first offset mirror for one photon energy.

	SASE1, D_{source}=437 m	SASE2, D_{source}=272 m
$l_{mirror}(4\sigma)$	700 mm	435 mm
$l_{mirror}(6\sigma)$	1050 mm	652 mm

Equation (3) assumes that the mirror angle is tuned to the critical angle of the particular energy. If the energy is then lowered without changing the angle of incidence, the larger beam divergence at lower energies leads to less than 4σ (or respectively 6σ) coverage of the beam profile. This is illustrated in figure 4, where the green curve describes the transmission of an 800 mm long SASE1 mirror at an incident angle of 1.5 mrad. At the cut-off energy of 18 keV it reaches more than 4σ coverage and one can tune the energy down to about 15.8 keV before the coverage becomes less than 4σ. At e.g. 12 keV only 3σ of the FEL beam is covered by the mirror. To achieve a better coverage, the mirror could be tuned to 2.2 mrad (red curve). For energies above 18 keV the reflectivity at 1.5 mrad goes to zero, so one has to reduce the angle of incidence (blue curve).

Figure 4 illustrates that a wider photon energy range can only be transmitted, if the angle of incidence at the offset mirrors is adjustable to the energy range. In the double mirror setup for the offset mirrors of SASE1&2 this can be achieved by lateral movement of the second mirror in the order of 10 cm perpendicular to the beam propagation direction.

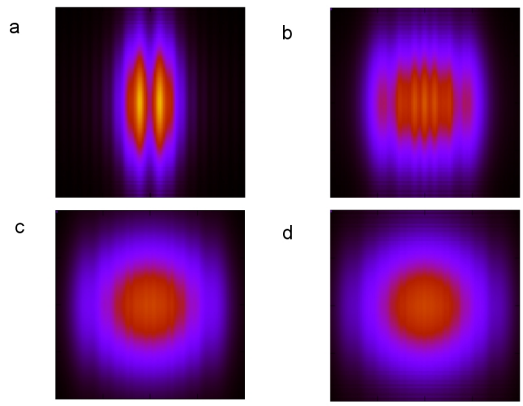

Figure 3: Wavefront calculations for the first offset mirror at SASE 1 for 12.3 keV as it would be observed in the experiment hall. The projected mirror lengths are 2σ (a), 4σ (b), 5σ (c) and 6σ (d). The field of view is 2 x 2 mm.

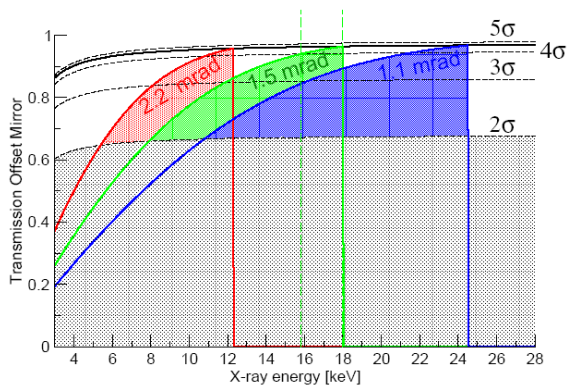

Figure 4: The transmission of an 800 mm long the first offset mirror at SASE1 for three different incidence angles. The dotted lines indicate the relative size of the footprint on the mirror. The grey area indicates less than 2σ footprint. The thick black line is the maximum transmission with optimized incident angle.

This will lead to a shift of beam position (figure 5, top). However, since the offset mirrors are more than 500 m away from the experimental hall, the beam position in the experimental hall can easily be kept constant by small adjustments of the reflection angle at the second offset mirror. This will lead to a small (0.2 mrad) variation of the beam direction in dependence of 'shifting' the second offset mirror, which has to be considered in the design of the X-ray optics in the experiment stations.

Distribution Mirrors

The beam after the two offset mirrors can propagate directly to the experimental station. However, within the space constraints of the X-ray tunnels, it is also possible to deflect the beam about 1.45 m left or right of the direct beam, which allows having up to three experimental setups side by side at the same undulator (figure 5, top). Even though it might be possible to operate two or three beamlines in parallel (e.g. by partial illumination of a distribution mirror or angular oscillation of the second offset mirror synchronous to the 10 Hz pulse train repetition rate), the main advantage of this beam distribution scheme is the possibility to prepare experiments in two stations, while one experiment takes data.

The reflection angle at the beam distribution mirrors is fixed once the position in the tunnel and the lateral separation of the beams are selected. Contrary to the offset mirrors, the incident angle can not be adjusted to the photon energy and beam divergence.

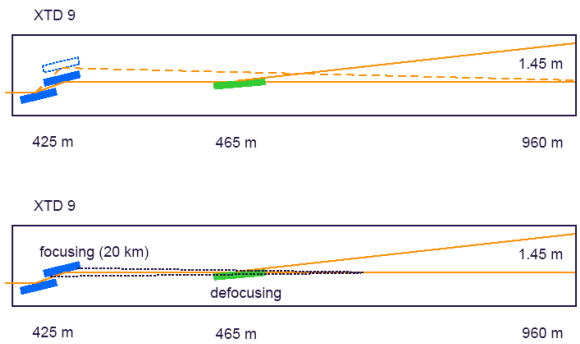

Figure 5: Beam distribution scheme. For clarity, only one branch beamline is shown. Top: Horizontal shifting of the second offset mirror allows for a variation of the reflection angle at the offset mirrors. Bottom: Focusing onto the distribution mirror can maintain the beam footprint above 4σ.

For the lower photon energies this would lead according to the above discussion to distribution mirrors several meters long. This length can be reduced by focusing the beam with the second offset mirror to an intermediate focus position behind the distribution mirror (figure 5, bottom). To vary the horizontal beam size at the experiment locations, the distribution mirror has to be bent convex.

The bending radii of the second offset mirror and the distribution mirror can be calculated as

$$\frac{2}{R_m} = \sin\theta \left(\frac{1}{p} + \frac{1}{q} \right), \qquad (4)$$

where R_m is the meridional bending radius of the mirror, θ the incidence angle, p the distance to the source and q the distance to the focus.

Optics Optimization

The presented scheme of beam offset and distribution mirrors requires an adjustment of all involved mirrors and re-adjustment of the bending radius of two mirrors, once the energy has to be changed over a larger range. The size of the energy intervals where no adjustment is required depends on the length of the available mirrors and the distance from the undulator. To obtain an optimization of required motions, mirror bending radii and sizes of energy intervals, a Matlab program has been used for ray-tracing different scenarios. Available mirror length, desired energy range, minimum desired bending radii, and the tunnel geometries are used as inputs, while mirror positions, angles, actual bending radii and size of energy intervals that require no shifting are the output parameters. A graphical representation of the output for the SASE1&2 beamlines are given in figure 6; the corresponding parameters are displayed in table 2.

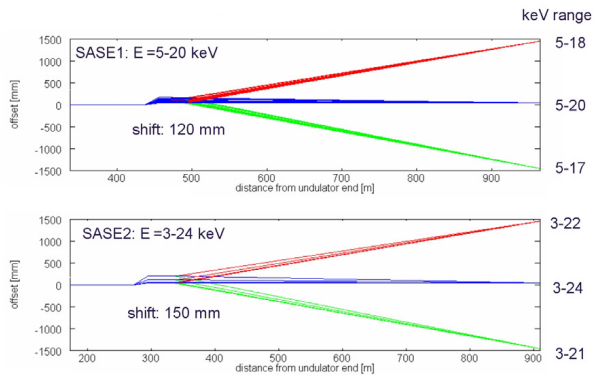

Figure 6: Graphical output of the ray-tracing optimization or SASE1 (top) and SASE2 (bottom) beamlines with 800 mm long mirrors.

From the optimization the following conclusions can be drawn:

- Operation up between 3-20 keV (SASE1) and 3-24 keV (SASE2) can be realized with the proposed optics scheme and 800 mm long mirrors.
- The required minimum bending radii of mirrors can be kept fairly moderate in the range of 20 km. This allows a fairly stiff mirror design for minimizing shape errors.
- At the SASE2 beamline the energy interval where no adjustment is needed is significantly larger than at SASE1, because the offset mirrors are closer to the undulator. With 500 mm long mirrors the situation at SASE2 is similar to the SASE1 photon beamline with 800 mm mirrors.
- The required lateral translations of the second offset mirror and the distribution mirrors are in the range of 100-200 mm.

Table 2: Beam line parameters after optimization. M1 and M2 are the two offset mirrors, M3 and M4 the distribution mirrors. ΔE is an average photon energy interval, where no re-adjustment is required; ΔX is the lateral translation needed at the second offset mirror for tuning through the entire energy range.

	mirror length [mm]	E[keV] central	E[keV] left	E[keV] right	ΔE [keV]	M1&M2 α[mrad]	M2 R[km]	M2 ΔX [mm]	M3&M4 α[mrad]	M3&M4 R[km]
SASE1	800	3-20	3-16	3-15	1.6	1.35 → 8	19 →∞	233	1.6 → 1.8	-24 →∞
		5-20	5-18	5-17	1.6	1.35 → 5	18 →∞	120	1.5 → 1.6	-20 →∞
SASE2	800	3-24	3-22	3-21	8.5	1.1 →5	18 →∞	150	1.2 → 1.4	-22 →∞
		5-24	5-23	5-21	8	1.1 →3	16 →∞	80	1.2 → 1.3	-17 →∞
	500	5-24	5-22	5-21	1.1	1.1 →5	18 →∞	150	1.2 → 1.4	-21 →∞

The upper cut-off energy of the branch beamlines are defined by available tunnel length after the distribution mirrors and desired beam separation in the experimental hall.

A summary of the available energy range at the hard photon beamlines and the intervals of shifting the mirror geometry is illustrated in figure 7.

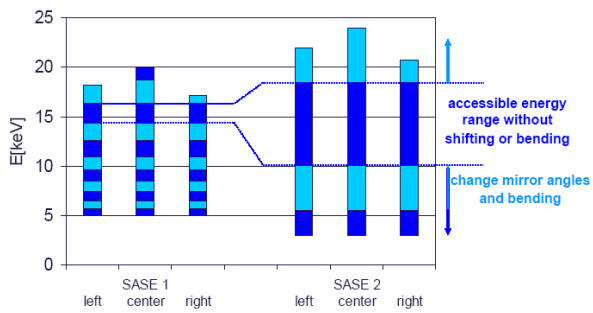

Figure 7: Energy ranges of SASE 1&2 photon beamlines. The light and dark blue colored areas can be accessed by 'shifting' the mirror geometry.

DAMAGE AND HEAT LOAD

A crucial question to be answered is whether the X-ray optics can survive the high X-ray peak power during a single pulse and the extreme heat load during pulse trains. On the other hand, the time averaged heat load of the hard X-ray FEL radiation is in the order of 30 W and the synchrotron radiation background in the order of 1 kW, which is smaller than heat load that can occur at storage ring sources. Removal of the average heat load is therefore typically no mayor concern and engineering solution similar to those developed for storage rings can be applied.

A critical threshold for the occurrence of single shot damage is reached when the local energy density in the material exceeds the melting. Above this threshold the material will ablate and at sufficient higher energy densities phenomena like plasma formation or non-thermal melting can occur. This situation is typically present in a micron-sized focus of the FEL beam. Except for the case of single shot optics, which is not discussed here, the peak energy concentration in all elements has to stay significantly below the melting threshold.

An estimate for the melting threshold W_{melt} per atom can be obtained by

$$W_{melt} \approx 3k_B T_{melt}, \quad (5)$$

yielding e.g. 1 eV/atom for diamond, 0.7 eV/atom for B_4C and 0.4 eV/atom for silicon. Since the heat capacity is here approximated in the high temperature limit and the initial thermal energy is neglected, these values can be considered as upper estimates. Also, the precise value might depend on photon energy, pulse duration, incidence angle and sample morphology [7, 8].

The volume, over which the pulse energy is initially distributed, is given by the footprint of the beam (beam size b_{fwhm}) on the optics element and the penetration depths perpendicular to the surface d:

$$W_{atom} = \frac{4\ln 2\ (1-R) W_{pulse}\, m \sin\theta}{\pi\, b_{fwhm}^2\, d\, \rho_m} \quad (6)$$

Equation (6) is normalized such that W_{atom} describes the maximum energy per atom with mass m, corresponding to a spot in the center of a Gaussian beam. The penetration depths d and the reflectivity R are given by

$$d = \frac{\lambda\varsigma}{4\pi\beta}, \quad (7)$$

$$R = \frac{\varsigma^2(\sin\theta - \varsigma)^2 + \beta^2}{\varsigma^2(\sin\theta + \varsigma)^2 + \beta^2}, \quad (8)$$

with

$$\varsigma = \sqrt{0.5\sin^2\theta - 2\delta + \sqrt{(\sin^2\theta - 2\delta)^2 + 4\beta^2}},$$

and δ and β are real and complex parts of the index of refraction n

$$n = 1 - \delta - i\beta.$$

A plot of the W_{atom} in figure 8 shows that the relative dose per atom is a constant at high incidence angles, has a

maximum at the critical angle and reduces significantly at smaller angles. Above the critical angle the variation in size of the beam footprint is compensated by the variation of the perpendicular penetration depth, which is in that case simply the photo absorption depth times the sine of the incidence angle. Below the critical angle, the penetration depth remains almost constant, so the increase of the footprint and the reflectivity lead to a sharp decrease of the dose at low angles. In this regime an even further decrease of the dose was observed due to transport of energy through fast photoelectrons [8], which is however neglected in eq. (7).

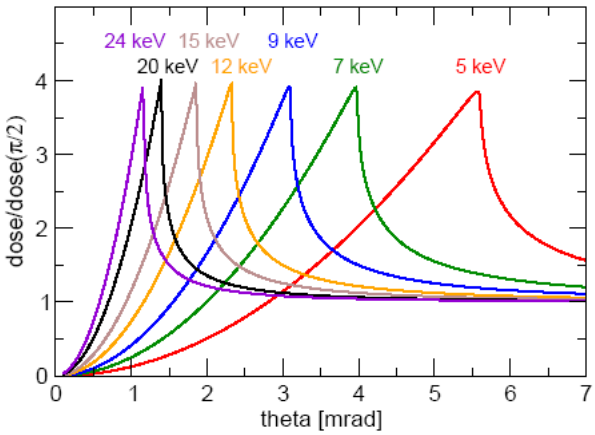

Figure 8: Dose per atom for B4C for different photon energies according to eq. (6). The scale is normalized to the dose at normal incidence.

With the incidence angles and the beam footprints calculated in the previous section, the dose per atom can now be estimated according to eq. (6) for a 1 mJ pulse (figure 9). For a 'worst case' scenario in terms of optics damage, the beam divergence was here assumed smaller than for the estimation of mirror lengths by setting the constant in eq. (1) to 11.6, corresponding to divergence values in [1]. Between the two hard X-ray beamlines, the offset and distribution mirrors of the SASE2 beamline will see the higher dose, because they are closer to the source. Even though the radiation is focused onto the distribution mirror, the dose is smaller, because it is operated for low energies significantly below the critical angle.

With pulse energies between 2 and 5 mJ at the hard X-ray SASE beamlines, the damage potential at the mirrors will be in the range of 1% of the melting threshold.

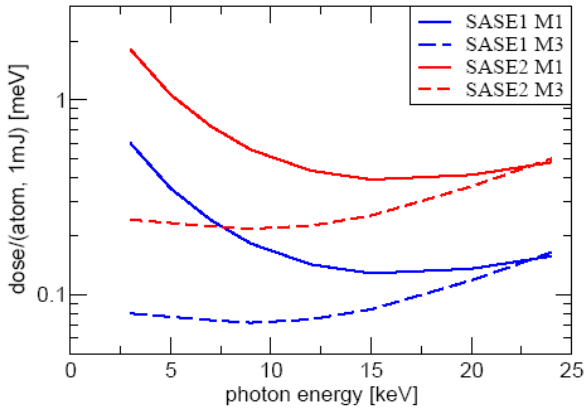

Figure 9: Dose per atom for offset and distribution mirrors on SASE 1&2 beamlines for a pulse energy of 1 mJ. Optical constants correspond to a B_4C coating.

Heat Load

Apart from the damage potential of a single pulse, the thermal energy of up to 2700 pulses can build up during a pulse train. During these up to 600 μs long time intervals, the average load on optical elements can easily exceed 10 kW/mm^2. Without removal of heat during a pulse train, practically no solid material is able to survive undamaged direct exposure to the XFEL beam for long pulse trains. At the mirrors, the temperature distribution is mainly one-dimensional, resulting in a heat flow perpendicular to the surface. Assuming a Gaussian-like initial temperature distribution, a time constant τ for the initial heat removal can be estimated by:

$$\tau = \frac{3d^2}{4\kappa} \qquad (9)$$

with κ being the thermal diffusivity [9]. For a silicon mirror substrate at room temperature κ=8.8 10^{-5} m^2/s and typical values of $d \approx 10$ nm in equation (7) for total reflection conditions. The derived time constant τ ≈ ps, much less than the spacing between x-ray pulses of 0.22 μs. Therefore, a significant part of the heat can be removed in between pulses, leading to moderate heat-up of the mirror surfaces of a few degrees during a pulse train. A resulting heat bump of several nanometers builds up during pulse trains deforms the wavefront of the beam slightly and can lead to small defocusing effects in subsequent optics [5, 10].

The average heat load on the mirrors from the FEL radiation is a few watts, which can be removed by water cooling. The first mirrors sees however also the spontaneous undulator radiation of 100 keV and higher. The power load on the first offset mirrors from this radiation is estimated in table 3. It can exceed 100 W, unless the mirror is protected by an aperture that absorbs most of less collimated spontaneous radiation.

Table 3: Calculation of spontaneous radiation heat load on the first SASE2 mirror after an aperture for an electron energy of 17.5 GeV.

FEL resonance	15 keV	5 keV	3 keV
Incidence angle	1.8 mrad	5.4 mrad	9 mrad
Beam size	0.4 mm	1.2 mm	2 mm
Aperture size [mm]	1.4 x 1.4	4.3 x 4.3	7 x 7
Transmitted power through aperture	8.54 W	11.28 W	31.6 W

The conceptual design for such a water cooled aperture is shown in figure 10

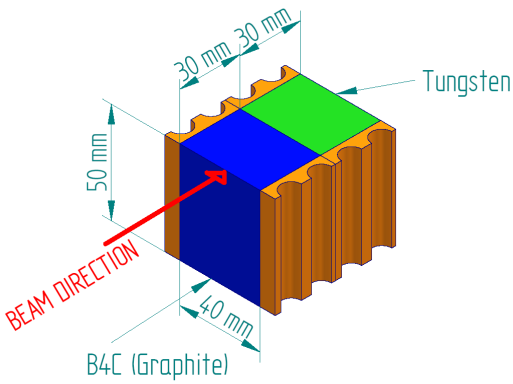

Figure 10: Conceptual design for one blade of an aperture in front of the first mirror. Water cooling is done through copper pipes brazed to the sides of the structure.

By careful setting of apertures around the FEL beam, the influence of spontaneous radiation can be limited and static temperature gradients can be kept around 1 Kelvin by water cooling of the mirror substrate (Figure 11). A small resulting convex bending of the mirror in the range of 100 km can be compensated by the bending mechanism on the second offset mirror. Suitable mounting and bending schemes are currently being investigated.

CONCLUSIONS

It was shown that with conservative assumptions on the FEL beam divergence a beam transport and distribution scheme can be realized with 800 mm long mirrors over a photon energy range of 3-24 keV for the two hard X-ray SASE beamlines of the European XFEL.

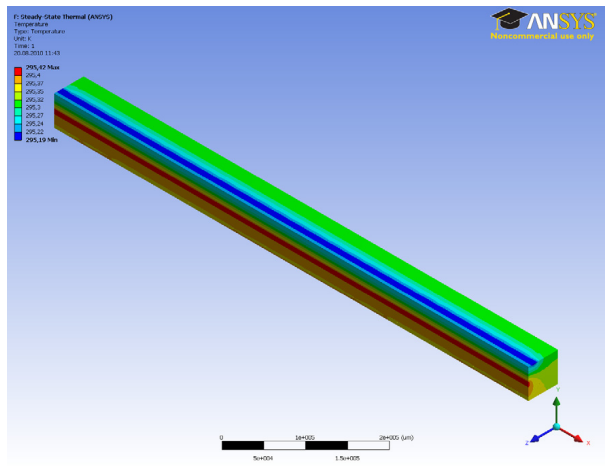

Figure 11: Temperature distribution of the first SASE 2 mirror after an aperture with water cooling on the top surface.

The minimum footprint on the mirrors is 4σ of the beam size. This requires an adjustment of reflection angles to the photon energy at the offset mirrors and focusing onto the distribution mirrors. Radiation from one pulse is in the range of 1% of the melting threshold. Averaged heat loads and heat loads during a pulse train lead in the grazing incidence geometry only to small deformations and can be controlled by water cooling.

REFERENCES

[1] M. Altarelli et al. (ed) The European X-ray free-electron laser *Technical Design Report*, DESY 2006-091 Hamburg (2006).
[2] P. Emma et al., Nature Photonics, DIO:10:1038/NPHOTON.2010.176 (2010).
[3] K. Yamauchi et al, Applied Optics, Vol. 44, Issue 32, pp. 6927-6932 (2005), and L. Samoylova et al, Proc. SPIE Vol. 7360, 7360-11 (2009).
[4] G. Geloni et al. Coherence properties of the European XFEL, New Journal of Physics **12** (2010) 035021.
[5] L. Samoylova et al., Preservation of coherence properties at hard X-ray beamlines of the European XFEL submitted to SPIE 2010 proceedings.
[6] M. Yurkov, private communications, DESY (2010) and poster MOPC05 at FEL2010 conference.
[7] S. Hau-Riege et al., APL **90**, 173128(2007).
[8] J. Chalupsky et al., APL **95**, 031111(2009).
[9] H. Sinn, Heat load estimates for XFEL beamline optics, Hasylab annual report 2007.
[10] F. Yang et al. Proc. Computational methods for coupled problems in science and engineering ECCOMAC thematic conference (2009).